Mon. Not. R. Astron. Soc. **000**, 1–14 (2006) Printed 6 February 2020 (MN LATEX style file v2.2)

Optimisation of the 3-body dynamics applied to extra-solar planetary systems

G. Windmiller[1⋆], D. Short[2] and J. Orosz[3]
[1] *Department of Astronomy, San Diego State University, San Diego, CA 92182, USA*
[2] *Department of Mathematics and Statistics, San Diego State University, San Diego, CA 92182, USA*
[3] *Department of Astronomy, San Diego State University, San Diego, CA 92182, USA*

Hopefully Accepted 2007; in original form 2006

ABSTRACT
The body of work presented here revolves around the investigation of the existence and nature of extra-solar planetary systems. The fitting of stellar radial velocity time series data is attempted by constructing a model to quantify the orbital properties of a star-planetary system. This is achieved with the Planetary Orbit Fitting Process (POFP). Though specific to the investigated problem, the POFP is founded on two separate, more general ideas. One is a Solver producing the gravitational dynamics of a Three-Body system by integrating its Newtonian equations of motion. The other is an independent optimisation scheme. Both have been devised using MATLAB. Applying the optimisation to the Solver results in a realistic Three-Body dynamics that best describes the radial velocity data under the model-specific orbital-observational constraints. Combining these aspects also allows for the study of dynamical instability derived from interaction, which is reaffirmed as a necessary criterion for evaluating the fit. The validity of POFP solutions with respect to the observations and other models is discussed in this context. The underlying generality and fundamental principles demonstrate a larger frame of operation where problems in Physics and Mathematics can be solved with a multitude of techniques.

Key words: planetary systems – celestial mechanics – gravitation – instabilities – methods: N-body simulations – methods: numerical

1 INTRODUCTION

One way to infer the existence of objects orbiting a star is by the use of the stellar radial velocity (RV) measurements obtained through the observation of the Doppler Shift in the star's spectrum. It can be shown (Windmiller 2006) that in a n-Body gravitational system in which the centre of mass (CM) does not accelerate, the secondary centre of mass of $n-1$ bodies tends to move with a momentum in the opposite direction to that of the other body, thus resulting in a reflex motion that has a component along the observer's line of sight. It is therefore possible to construct a model in which the stellar motion in the radial direction is calculated based on the gravitational dynamical interaction of the bodies in such a system. Numerous stars have been surveyed to date by different observing groups (UCLES Keck/Lick, HARPS/CORALIE, The AAPS...) using high resolution velocity measurements of each star with planetary bodies either determined or conjectured. The method of analysis of these radial velocity data has been outlined in several papers over the years (Laughlin 2001, Rivera 2005, Pepe 2006) and has slowly evolved with the essential features remaining unchanged. The first step in the analysis is the determination of Keplerian orbital parameters under the assumption of no mutual gravitational perturbations between the planets, eliminating any significant periodicities in the residual. Once the number of conjectured planets - each with its own Keplerian parameters - has been determined, additional assumptions such as co-planarity, edge-on orbits, or resonance, are used to arrive at a full set of Newtonian initial conditions. This orbital configuration is then used as the initial guess for a quasi-Newton's method search (usually the Levenberg-Marquardt algorithm). The restriction of no mutual planetary gravitational interaction is lifted, and the search proceeds to a self consistent local minimum in the parameter-space vicinity of the Keplerian orbital fit. Using this family of methods, only a local minimum close to the Keplerian parameters under the specific restrictions will be found.

The alternative model proposed here for the prediction of stellar RV data relies on a direct integration of the Newtonian equations of motion for a Three-Body gravitational

⋆ E-mail: windmill@rohan.sdsu.edu

interaction. The developed RV reduction algorithm constituting this model encorporates the assumption that in general, there will be significant mutual gravitational planetary perturbation, since it is exactly the star's reflex action to the planetary presence that is being measured. Searching the full set of possible initial conditions while directly integrating allows for the investigation of all orbital pathologies unconstrained by any factors (such as co-planarity, resonance, etc.). Each solution, which is the set of initial conditions for the single integration of Three-Body trajectories and velocities is put in the form of a 12-*tuple* of orbital parameters. Once the full Newtonian trajectories are calculated, an algorithm based on the Singular Value Decomposition finds the optimal orientation based on the RV data set. In order to find a solution which predicts a RV curve that sufficiently matches the observations, an optimization process based on methods from the literature has been devised. The search for the absolute minimum of the χ^2 is implemented first with a Genetic Algorithm, then with a local search method, typically a Compass or a quasi-Newton's method. The entire process of analyzing and predicting the RV data, is referred to here as the Planetary Orbit Fitting Process (POFP). All of the algorithms described here are written in MATLAB, utilizing its versatility as a mathematical computer language, and a working platform with a graphical interface and powerful application packages. These include diverse tools such as the suite designed to integrate and manipulate Ordinary Differential Equations (ode). Because the POFP in its entirety was not previously described in the literature, a comprehnsive description is included here, complimented by the appendices for more detail. The Three-Body **Solver** at the centre of the POFP is described in §2. The application of the **Solver** to produce a predicted stellar RV time series via the orbital-observational parameters is described in §3. A brief description of the optimization scheme follow in §4. Considerations involving the comparison between predicted and observed quantities are discussed in §4 as well. The Keplerian model which is the basis of the methods currently used throughout the literature, orbital stability considerations and the connection between the two are discussed in §5. Applications of the POFP using the published radial velocity data for the HD160691 and HD141929 systems are demonstrated in §6 and other cases are discussed in future papers.

2 THE SOLVER

The gravitational interaction between N bodies due to Newton's Second Law and the Universal Law of Gravitation is given by the system of equations

$$\ddot{\boldsymbol{r}}_i = -G\left[\sum \frac{m_j}{{\boldsymbol{r}_{ij}}^2}\right]_{i\neq j}, i,j = 1 \rightarrow N \qquad (1)$$

where m_j is the mass of particle j applying force on particle i from a relative position $\boldsymbol{r}_{ij}$. In the case of three bodies in three dimensions, $N = 3$, and $\boldsymbol{r}_i = (x, y, z)$ is the displacement vector of particle i. Assuming the CM of the system moves with constant velocity, one of the vectors in system (1) can be expressed in terms of the other two:

$$\ddot{\boldsymbol{r}}_3 = \frac{m_1\ddot{\boldsymbol{r}}_1 + m_2\ddot{\boldsymbol{r}}_2}{m_3} \qquad (2)$$

where $\ddot{\boldsymbol{r}}$ is the acceleration vector in the CM frame. The system (1) then consists of six second order, or twelve first order differential equations of motion. The initial conditions for this system are the three masses and their initial position and velocity vectors.

It is then integrated for the trajectories $\boldsymbol{r}_i(t_i)$, and velocities $\boldsymbol{v}_i(t_i)$ utilizing the MATLAB ODE suite. The algorithms chosen from the suite were ode113 (Variable order Adams-Bashforth-Moulton) and ode 45 (Runge-Kutta-Fehlberg, Dormand-Prince pair). The time span for integration, the relative and the absolute tolerance were specified along with the initial conditions. As part of this scheme, interpolation can be made over the integrated interval to any desired step size[1] allowing for no further integration. The **Solver** has been tested on problems with known solutions to make sure of its proper use. With the integration of every orbit, the angular momentum is calculated for each time step and the relative error in it throughout the entire integration time is computed to show conservation. Using the constants defined to great accuracy by the IAU[2], and data tabulated in Nautical Almanac Office (2006), the trajectories of the Earth-Moon Barycentre, the Earth-and-Moon and the Earth-and-Jupiter systems around the Sun were computed. The orbits were shown to close (in distance and time) to a sufficient accuracy compared with that of the initial data (Windmiller 2006). All orbits showed the conservation of angular momentum to the number of digits defined by the error-tolerance. The trajectories calculated by the **Solver** have no specific orientation towards an observer. To define the direction of the observer's line of sight, the **Solver's** coordinate system must be rotated (see Appendices B,C).

3 APPLICATION OF THE SOLVER TO A PLANETARY ORBITAL MODEL

The application of the Three-Body solutions (trajectories and velocities as a function of time) produced by the **Solver** to the problem of fitting an observed stellar RV variation, is made through the assumption that two of the masses (planets) are orbiting the third (star). The search of the full set of initial conditions for the Newtonian equations of motion must bring into account the fact that any random set of such conditions most likely leads to unbound trajectories. To resolve this problem, the set of feasible initial conditions can be parametrized by the set of instantaneous Keplerian parameters at the time of the initial data point. Masses, eccentricities and angular information as to relative positions of the orbits and their periastra are used for this parametrization. The result is a set of orbital parameters from which the initial conditions for the orbiting masses in their two graviataionally bound trajectories are calculated.

In the plane of each orbit, the initial position and velocity vectors are defined with respect to the point of periastron, using the eccentricity, e, and a '*delay*' angle, θ, measured from the semi-major axis (see Appendices A,E). Given the relative positions of the two semi-major axes and

[1] Details on the workings of the ode suite can be found in Shampine et al. (2003)
[2] http://193.49.4.189/Units.234.0.html

the relative tilt between the orbital planes, the initial positions and velocities of one orbit can be transformed into the coordinate system of the other so that all quantities are defined in the same system. This transformation is achieved by a multiplication of three rotation matrices in which the angles are defined by the relative coordinates of the semi major axes (see Appendix A). These nine orbital parameters allow for any possible geometry of the two planets orbiting the star at the epoch of initial conditions. The observer's coordinate system is defined as one where the (x', y') plane is the plane of the sky and the z' is the radial direction. The orientation of the **Solver's** coordinate system to the observer's line of sight can be defined using two angles. One of the orbits is chosen and its inclination, i, and longitude of periastron, ω are used to transform the coordinate system of the **Solver** into that of the observer. This transformation is also the product of two rotation matrices (Hilditch 2001). The orbital parameters that are therefore sufficient to define the initial conditions to the **Solver** for the planetary model are the eccentricities $e_{1,2}$, the delay angles $\theta_{1,2}$, the length of the first semi-major axis x_1 and the coordinates of the second semi-major axis (x_2, y_2, z_2), the relative orbital tilt angle τ, and the three masses m_1, m_2, m_3. The observational parameters required are the inclination i and the longitude of periastron ω. Parameter-space for any n-tuple of initial conditions satisfying the Three-Body requirements of the **Solver** has fifteen dimensions. This 14-tuple of planetary-model parameters thus reduces by one the number of dimensions in which the search for initial conditions must take place.

The number of dimensions can be reduced further to include the 12 orbital parameters only. For any orbital configuration defined by the parametric 12-tuple, the observer's position (i.e. i and ω) from which the **Solver**-frame stellar velocity best describes the RV data can be calculated. The calculation is based on optimizing a least square solution for a unit 'look vector', defined by the two angles, which points from the CM of the stellar system to the observer. The matrix equation is solved using the singular value decomposition (utilizing MATLAB's *svd* function) applied on the star's velocity in the **Solver** frame (see appendix C).

4 OPTIMISATION AND THE FITNESS FUNCTION

To find the parameter-point (14-tuple or 12-tuple) for which the comparison between the model-predicted and the observational data results in the absolute minimum χ^2, an optimization process was carried out in two steps[3]. The first step is the implementation of the Genetic Algorithm (GA) as a global search for the region in parameter space where the lowest χ^2 lies. The second step of refining the search to the exact parameter-space location of the absolute minimum in the χ^2 was carried out in various ways. Of the derivative-based methods, the linear slope and the quadratic slope methods were found to be the least efficient. This is because of the rapid change in the fitness function's slope and numerical-derivative noise problems (Windmiller 2006). The Hybrid Newton-line search method was typically used to advance the search quickly where other methods were unsatisfactory. The second-step method most frequently used was the Compass search. All algorithms were constructed as independent MATLAB programs. The programming of the GA followed several discussions in the literature[4,5]. The compass was based on Kolda, Lewis & Torczon (2003). All methods used, most specifically the GA and Compass, were tested against known analytical functions before their use in the POFP.

To produce the predicted radial velocity data, the POFP implements two translation processes. First, the n-tuple of parameters is translated into initial conditions for the **Solver**. The information about the dynamical properties of the system (in the form of the solution produced by the **Solver**) then undergoes a translation into the observer's plane of the sky coordinate system. An n-tuple of parameters therefore constitutes a single hypothesis that a specific configuration of initial conditions results in a model that is compatible with the observations. The quantification of this level of compatibility is made via a fitness function. The specific fitness function used by the POFP is the χ^2 (Chi-Squared). The derivation and treatment of the χ^2 function follows that of Bevington & Robinson (2003) and Press et al. (1992). The assumption that the CM of the stellar system does not accelerate allows for a constant offset velocity to be incorporated into the χ^2 function (such a fitness function is presented in Goździewski & Maciejewski (2003)). The optimal offset velocity is calculated in closed form within each evaluation of the χ^2 (appendix D). Because of technical considerations and as the standard used in the literature, the form of the fitness function that is used in practice is the reduced Chi Squared, χ^2_ν, (with ν being the number of data points minus the number of parameters, or degrees of freedom, plus 1). The expected value of χ^2_ν is ≈ 1. However, because this exact value typically is not achieved, a range of values must be considered. One approach in the interpretation of the POFP solutions' χ^2_ν is based on using the F test as suggested in Press et al. (1992). Given $\chi^2_{\nu_1}$ and $\chi^2_{\nu_2}$ it is not possible to reject the assumption that both represent the same data set if both reside inside the same interval. This interval is determined as a confidence measured by a probability which is given by the appropriate integral-test probability table. For a desired probability of not exceeding the ratio $F = \chi^2_{\nu_1}/\chi^2_{\nu_2}$ (typically a probability measuring the confidence of one standard deviation), the ratio can be calculated, considering the numbers of degrees of freedom $\nu_{1,2}$. Press et al. (1992) provides the expression for calculating the ratios as a function of the probabilities. This interpretation allows for both a comparison between any two values of χ^2_ν (provided ν is similar in both and sufficiently large) and a determination of the range of values in which solutions are acceptable relative to one another.

When considering the acceptability of a given solution produced by the POFP, the χ^2_ν is treated as the primary criterion. The secondary measure for how well the fit describes the observations is the Root Mean Square (RMS) of

[3] All algorithms discussed here were developed by Donald Short

[4] Houk, Joines and Kay: http://www.ie.ncsu.edu/mirage/GAToolBox/gaot/papers/gaotv5.ps

[5] Parker: http://pharos.cpsc.ucalgary.ca/Dienst/Repository/2.0/Body/ncstrl.ucalgary_cs/1995-564-16/pdf

the error, along with the distribution of the residual velocities which is expected to be a Gaussian centred at zero. In the framework of the POFP, a useful RMS-related quantity is $\mathrm{RMS_{ERR}} = \sqrt{\sigma_{\mathrm{res}}^2 - \sigma_{\mathrm{jit}}^2}$. Here, σ_{res} is the standard deviation in the residual velocities (comparable to the RMS in the literature) and σ_{jit} is an uncertainty added to the observed velocities due to a variety of factors largely unknown and, in part, related to stellar chromospheric activity (Wright 2005). The latter is termed here Jitter. Apart from considering its magnitude, the quantities RMS and $\mathrm{RMS_{ERR}}$ can be compared to the uncertainty in the observed data. The quantification of the fit by the χ^2_ν and the RMS may yet be insufficient for determining how well the model describes the observed phenomenon. One of the most important considerations that typically applies is that of stability. As the investigation using the POFP of the 47UMa system (described in Paper II), as well as that of HD160691 show, solutions that have a low χ^2_ν may also ascribe a large eccentricity to one of the planets, resulting in instability. Dynamical stability of the system, therefore, must be considered as a tertiary criterion for accepting the fit.

5 THE KEPLERIAN MODEL AND STABILITY

The application of the POFP is demonstrated in §6 on the star systems HD160691 and HD141929 which have previously been investigated in the literature. In order to reproduce published results that are based on a Keplerian model, a similar scheme has been developed as part of the POFP programming. Separate from the Planetary Model described earlier, this Keplerian Constants (KC) model allows for a confirmation or an evaluation of the published Keplerian results and a comparison between those and the ones produced by the POFP.

5.1 The Keplerian Constants Model

The classical Keplerian model that has been programmed here is termed the KC model. It is based on the equations derived for binary mechanics as found in any standard textbook (e.g. Hilditch 2001) in relation to the general analytic Two-Body solution and is comparable to that commonly used in the literature. In this model, the motion of a mass in an elliptical orbit around a second mass (here a planet around a star) as a function of time is described by Kepler's equation. Using the period, P, and the periastron passage time, T, this equation relates the Mean Anomaly $\Theta = 2\pi(t-T)/P$ of the orbiting mass to its Eccentric Anomaly, E, and the eccentricity of orbit, e:

$$\Theta = E - e\sin E \tag{3}$$

The program iterates (using the Newton Raphson method) for the Eccentric Anomaly. The true anomaly (delay angle), θ, is calculated as a function of time:

$$\theta(t) = 2\arctan\left[\sqrt{\frac{1+e}{1-e}}\tan\left(\frac{E(t)}{2}\right)\right] \tag{4}$$

Using the Half Amplitude of the observed velocity, K, and the Longitude of Periastron of orbit, ω, the radial velocity can be predicted:

$$V_r(t) = K\left[\cos\left(\theta(t)+\omega\right) + e\cos\omega\right] \tag{5}$$

The predicted radial velocity is calculated separately, using Equation (5), for the influence of each planet on the star. These contributions to V_r are then superimposed to give the total predicted radial velocity. The planets are therefore assumed to have no interaction, making the Keplerian quantities constant in time. A parameter-point constituting a solution in this model is the n-tuple of KC $(K, P, e, T, \omega)_j$ with j designating the planet (i.e. the 5-tuple $j = 1$ for a single Keplerian, the 10-tuple $j = 1, 2$ for a double Keplerian, etc.). The appropriate parameter-point which minimizes the χ^2_ν can be searched for using the optimization scheme described in §4. As with the POFP, the GA is typically used as a first step, followed by the Compass method. When optimizing, the KC model is highly sensitive to the initial guess (or initial population).

POFP integration over a sufficiently long time span (typically much longer than that of the period of the outer planet) can expose a system as being dynamically unstable or prone to instability. This is done directly by showing an ejection of one of the bodies from the system, or at the very least a strong gravitational influence of the two planets on one another, making noticeable changes to their trajectories. Because the KC model assumes no gravitational interaction outside that between the star and each planet, a separate analysis for stability is required where other factors, not inherent to the model, are brought into account. An example of a discussion involving this type of analysis can be found in Goździewski & Maciejewski (2003). Using the **Solver** to compute the trajectories makes for a direct integration of the Newtonian equations of motion which is general in its underlying assumptions, and geometry. Because of that, a translation of the initial conditions of the KC model into those of the POFP, followed by integration based on the latter, may be useful in approaching the problem of orbital stability.

5.2 From Keplerian to POFP

The KC parameter point $(K, P, e, T, \omega)_j$ used by the model to express the orbital properties of the j^{th} planet as they appear to an observer through the plane of the sky (i.e. in the form of stellar RV data), describes a family of Newtonian solutions, each being an orbit initiated by a different set of position and velocity vectors. These solutions differ from one another by two parameters. The first is the planetary mass traveling in each orbit which can alternatively be expressed by the inclination of that orbit (using P, K, e and the mass of the star). For any two orbits, the second quantity is the difference in their position angle of the nodal point, (usually designated by Ω). Therefore, the Newtonian fit for any Keplerian solution can be described by the χ^2_ν calculated as a function of the masses or inclinations of the planets and their differences in position angles. Because the POFP's primary use is in solving for three-body trajectories, a rigorous analysis of the special case of two planets lends itself as a first step in understanding the relationship between the different models. Given the stellar mass, a 10-tuple of double Keplerian parameters (i.e. 10 KC) can be translated into the POFP 12-tuple of parameters, excluding the planetary masses. The χ^2_ν for such a solution can then be

calculated for triplets of $(i_1, i_2, \Delta\Omega)$, i.e. for pairs of masses (m_1, m_2) and their orbits' relative positions in the plane of the sky. As a preliminary analysis of this three dimensional parameter space, a crude optimization can be made where the $\Delta\Omega$ that minimizes the χ^2_ν for each pair of masses is chosen. The resulting surface, $\chi^2_\nu = s\,(m_1, m_2)_{\Delta\Omega_{\min}}$ can then be examined. For the entire span in inclination, the domain of this surface shows the allowable range of masses the particular Keplerian solution can have. The regions of lower χ^2_ν may easily be located on this surface, and the stability of solutions represented by specific points in them can be investigated. The principal idea of such an analysis through a translation is shown here in §6 for the double Keplerian as it applies to the test case of HD160691. Some detail of the translation is given in appendix E. A more rigorous stability analysis based on these methods will be discussed in a paper to follow.

5.3 Investigating Stability

One qualitative argument regarding interaction in a stellar-planetary system is the following: if a gravitational influence of the outer planet on the star exists (one that is sufficiently strong to be detected) then such an influence of the outer planet on the inner planet must also occur, causing the planets to interact, provided that the two are on the same side of the star. Concretely, in order to assess whether the trajectory calculated from a set of initial conditions results in an ejection of one of the bodies, or more generally, is prone to instability, the **Solver** can be used to integrate the orbit on a sufficiently large time span. Such an evaluation, based on the graphical representation of the trajectories, was carried out for all of the POFP solutions in Table 1 and Table 2 discussed in §6. The typical time span used was on the order of hundreds of times the larger period of the two planets. The assessment, using this method, of a possible instability of an orbital configuration requires a large degree of intuition on the one hand, and is limited by computational resources on the other hand. Because of that, the Hill stability condition was applied as a complementary criterion, following Gladman (1993). In his paper, Gladman (1993) distinguishes the Hill stability, where the bodies are forbidden from undergoing close approach for all time, from the stronger Lagrange stability where, in addition, the semi-major axes are bounded. The author defines closest approach, which is regarded by him as instability, as being inside the sphere of influence of the outer planet where "...it is better to view the motion as one planet around the other being perturbed by the 'Sun' rather than the planets moving around the Sun and being perturbed by each other" (Gladman 1993). The cutoff for this closest approach is defined numerically by the author in terms of the planetary mass ratio. As is the case in Gladman (1993), the approach taken here for establishing the Hill instability relies on the parametrization of the Three-Body dynamics by Marchal & Bozis (1982) in terms of the three masses, the gravitational constant, the angular momentum and the total energy of the system. For the case where two of the bodies are much smaller in mass than the third one, the critical value of this parametric expression, indicating a bifurcation of the system's dynamics, is computed by Marchal & Bozis (1982) in terms of the masses alone. The difference between the Hill number of a particular solution (i.e. the dynamical parameter of that orbital configuration) and the Hill critical value is referred to here as the Hill difference. When the Hill difference is positive, the planets are forbidden from having a disruptive close approach, which means the system is Hill stable (although ejection of the outer planet may still occur). Fulfilling the Hill condition is stated by Gladman (1993) to be sufficient but not necessary for overall stability in the system's dynamics.

6 DEMONSTRATING THE POFP APPLICATION

The case of the double-lined binary HD141929, observed and investigated by Carrier (2002), was used to show how the POFP treats a degenerate Three-Body structure. The analysis of this stellar system included a reproduction of the published results using the KC model, at least two viable Newtonian solutions competing with the published and reproduced ones, an error analysis on all solutions, and a χ^2_ν surface showing the expected stability properties of the system. Because the process was started with as few assumptions as was possible about the system (such as the stellar mass of the primary derived from its spectral type), a relatively general initial population was given to the GA. The solutions produced were all in the form of a translating binary with a small third mass at a distance, typically ejected from the hierarchy. These solutions can then be optimised further with the third mass set to an insignificant value. The error analysis of the KC reproduction, showing values close to the published ones is showin in Table 3. Some of the main results for this system are shown in Table 4.

6.1 An application to the star HD160691

To demonstrate the intricacies of the POFP analysis and its intepretation, the more complex case of HD160691 was chosen. Although more RV data of this system have accumulated since the publication referred to in this paper, the case of HD160691 is brought as an example of an analysis which is both comperable to other publications at a given point of time, and a work in progress. Some of the conclusions eminating from this analysis, especially in light of the new data, allow for the exploration of new directions in research.

The RV observations of HD160691 and a double Keplerian fit to these data are provided by McCarthy et al. (2004). The authors discuss stability analyses done by Bois et al. (2003) and Goździewski & Maciejewski (2003). Tables 1 and 2 here show the published result, its Keplerian reproduction, and the POFP solutions for this star, in a form compatible with the literature. For all solutions generated here, it is assumed that the data were taken using a single instrument. Table 1 contains the stellar mass and the quantities for the first planet, along with the χ^2_ν and RMS of each fit[6], and the stellar offset velocities. Table 2 contains the properties of the second planet and comments regarding both planets. In all of these solutions, the stellar mass

[6] The RMS for the solutions presented here is the standard deviation of the residual, ($\sigma_{\rm res}$) without subtracting the uncertainty due to jitter ($\sigma_{\rm jit}$) from it, making it higher than $\rm RMS_{ERR}$ discussed in §4.

was not allowed to vary by more than 15 percents from the published value of $1.08 M_{\odot}$. The maximum radial velocity for each planetary mass $m_{\rm p}$ around the star was calculated as

$$V_{r_{\max}} = \frac{G m_{\rm p} P \sin i}{2\pi a^2} \ .$$

.

Solution #1 is that published by McCarthy et. al. (2004). Using the solution's published parameters in the KC model described in §5.1, without including any jitter in the uncertainties, results in $\chi^2_\nu = 385$ with RMS = 47.7. Solution #2 is a reproduction of solution #1 using the KC model and applying the optimization described in §4. The published parameters (yielding solution #1) are used as a basis for an initial population and the GA followed by the Compass are implemented to find the minimum in the fitness function, with a result of $\chi^2_\nu = 1.27$ with 3 m/s jitter, or $\chi^2_\nu = 2.7$ with the jitter removed, and RMS = 4.2. The high χ^2_ν in solution #1 could be attributed to an error in one or more of the published parameters, most specifically the published value of the periastron passage of the first planet. Substituting this value with the guess, T = 260, based on the optimization in solution #2, yields a new $\chi^2_\nu = 1.26$ with 3 m/s jitter or $\chi^2_\nu = 2.68$ ($\chi_\nu = 1.63$) without any jitter, and RMS = 4.15. The published solution is therefore adequately reproduced.

Solution #3 is the first one listed that was generated by the POFP. With a $\chi^2_\nu = 1.44$ and a RMS = 4.30, it shows an agreement with the McCarthy et al. (2004) parameters for the first planet. Comparing the fit of solution #3 to that of the reproduction solution #2 (both include the 3m/s jitter in the data) shows the χ^2_ν of #3 to be larger than that of #2. However, as explained in §4 and is shown in Table 5, the two χ^2_ν values are well within a 1σ interval of one another. The RMS of #3, a measure of the fit which does not depend on the size of the error bars, is also larger than that of #2. The small negative Hill difference for this case could indicate instability. The solution was integrated over a time span of 400 times the larger planetary period. Examining the plot shows the trajectories to have a possible instability, i.e. not a definite ejection of one of the objects, yet a relatively large degree of interaction that may be disruptive subsequently. The period of the second planet in #3 is larger than that of #2 and the eccentricity much smaller. Nevertheless, it is possible that the large mass of the first planet, $M_{\rm p_1} \cong 63 M_{\rm J}$ is what makes this solution prone to instability.

Solution #4 demonstrates further the importance of considerations other than the χ^2_ν and RMS in establishing the viability of a model. The χ^2_ν in #4 is lower than that of the other POFP fits. The RMS, is as low as that of the other POFP cases (and lower than that of the Keplerian reproduction, solution #2). However, when integrating over a time span of over 50 times that of the longer planetary period, the trajectory shows an ejection of one of the planets due to a cumulative effect of planetary interaction. This instability is also exemplified by the negative Hill difference. The tradeoff between stability (in this solution, related to the relatively high eccentricity of the second planet) and lower χ^2_ν requires knowledge of the former in order to evaluate the latter. (This aspect of the model is treated by McCarthy et al. (2004) when discussing the stability analysis of the HD160691.)

Solution #5, with $\chi^2_\nu = 1.36$ and RMS = 4.18, is an example of a co planar solution. Co planarity can be enforced during the POFP by limiting the z_2 axis of the second planet and the tilt of its orbit, τ (see appendix A). The positive Hill difference shows the solution to be possibly stable, which is in agreement with an integration over 400 times the longer planetary period. The agreement with the parameters for the first planet of solutions $\#1 - \#2$ is apparent. The period of the second planet in this solution is 1.56 times that of the second planet in solution #2. The second eccentricity in #5, $e_2 = 0.226$, is about 0.4 that in #2. The combination of relatively low χ^2_ν and RMS, and apparent stability makes this a viable solution.

Solution #6 has a $\chi^2_\nu = 1.44$ and a RMS = 4.18. Unlike solutions $\#3 - \#5$, this one has been fitted using the entire 14-tuple of both orbital and observational parameters (see §3 and appendix C). Integration of this three-dimensional solution over 400 times the longer planetary period shows an apparent stability. This is supported by the positive Hill difference for this case. As in the other POFP cases, the parameters for first planet in this solution are in agreement with those of McCarthy et al. (2004) found in solutions $\#1 - \#2$. The period of the second planet in #6 is 2.8 times that of the second planet in #2 while the eccentricity of this planet in #6 shows a nearly circular orbit.

Solution #7, with a $\chi^2_\nu = 1.39$ and RMS = 4.25, is not coplanar, having a relatively small angle of 5° between the two orbital planes. As with the previous POFP solutions, this one also agrees with the parameters published and reproduced, for the first planet. The second planet has a period 2.05 times that of the second planet in #2 and an eccentricity of 0.12, making for a more circular orbit. An integration over 1000 times the longer planetary period shows this solution to be highly stable, a property supported by the positive value of the Hill difference. Fig. 1 shows the fit for this solution to the RV observations (where jitter has been included in the error bars). Fig. 2 shows a plot of the orbits integrated by the **Solver** around the CM of the system over a time span of 1 period of the outer planet. A plot of the orbit integrated over a time span of 400 times the period of the outer planet is shown in Fig. 3. The optimized look vector is shown as a red arrow stemming from the CM and the initial velocities as vectors stemming from the initial position of each orbit.

Solutions #8 and #9, show an agreement with the parameters for the first planet in all of the other POFP solutions. With similar periods for the second planet, they differ mainly in its orbital eccentricity values. The similar Hill difference values in the two solutions attest to the comparable behavior in orbital stability that is shown by direct integration of 1000 times the longer planetary period. Inspection of the plots of these trajectories shows the two planets interacting in a manner that is inconclusive in that it may be bordering instability. Using features in MATLAB that allow a presentation of the calculated trajectories as a function of time (i.e. in animation form) shows the orbits change their positions with respect to the star, but overall do not interact to the point of disruption. In that respect, it is interesting to note that the χ^2_ν and RMS are higher in #8, than in #9, possibly exemplifying higher stability which would be compatible with the higher Hill difference. If stable, the nearly coplanar #9, with $\chi^2_\nu = 1.36$ and RMS = 4.18, is a highly

Table 1. HD160691b (First Planet)

Solution #	Solution Type	Star Mass ($M_\odot$)	P (days)	e	a (AU)	$M \sin i$ (M_J)	$MaxV_r$ (m/s)	χ^2_ν	RMS[a] (m/s)	OV[b] (m/s)	Hill$_\#$-Hill$_{cr}$[c]
1	Published[d]	1.08	645.5	0.200	1.50	1.67	38.0	2.56[e]	4.66	–	–
2	Kep Rep	1.05	642.4	0.200	1.47	1.63	37.7	1.27[f]	4.20	–	–
3	POFP	1.10	642.0	0.179	1.53	1.72	36.7	1.44	4.33	-15.4	-0.01
4	POFP	1.05	646.7	0.185	1.52	1.74	37.8	1.34	4.15	-10.2	-0.04
5	POFP	1.06	642.6	-0.198[g]	1.49	1.65	37.3	1.38	4.18	-22.0	0.23
6	POFP	1.08	642.2	0.192	1.50	1.69	37.7	1.44	4.18	-68.9	0.60
7	POFP	1.08	642.0	0.183	1.49	1.68	37.5	1.39	4.25	-27.8	0.43
8	POFP	1.09	643.0	0.175	1.50	1.70	37.6	1.41	4.27	-21.5	0.25
9	POFP	1.08	642.9	0.202	1.50	1.70	37.6	1.36	4.18	-20.1	0.20

[a] For the generated solutions, #2 - #9, RMS $= \sigma_{\rm res} = \sqrt{\rm RMS^2_{ERR} + \sigma_{jit^2}}$
[b] Offset Velocity (calculated as part of the χ^2_ν)
[c] The Hill difference which is the critical Hill stability value subtracted from the Hill stability number for this solution
[d] McCarthy et al., 2004, ApJ 617, 575M
[e] The value published is $\chi_\nu = 1.6$, assuming no jitter.
[f] This solution includes 3 m/s jitter. Removing the jitter results in $\chi^2_\nu = 2.7$ (or $\chi_\nu = 1.64$). Refer to §6.1 and §6.2.
[g] the sign of the eccentricity determines whether the apsis position (the length of which is the numerator in equation A3) is an apastron or periastron.

Table 2. HD160691c (Second Planet)

Sol' #	P (days)	e	a (AU)	$M \sin i$ (M_J)	$MaxV_r$ (m/s)	i_1 (degrees)	i_2 (degrees)	Comments
1	2986	0.57	4.17	3.10	51.0	–	–	publication[a] may contain an error
2	2977	0.56	4.09	3.44	47.7	–	–	Double Keplerian
3	3616	0.02	4.76	1.85	23.0	1.60	52.6	Uncertain Stability, large first-planet mass[b]
4	5593	0.68	6.27	1.75	19.4	1.30	61.0	Unstable, large first-planet mass[c]
5	4657	0.23	5.58	2.73	31.9	12.6	12.6	Stable, Co-Planar
6	8315	0.00	8.26	7.87	74.6	22.4	90.0	Stable, 3D, Optimized with 14 parameters
7	6131	0.12	6.73	2.95	31.0	72.7	76.8	Stable, 3D (5° between orbital planes)
8	4991	0.15	5.89	2.48	27.7	17.8	69.4	Stable (or semi-stable)
9	4984	0.26	5.88	2.51	28.2	07.0	18.4	Stable, slightly large planetary masses[d]
								All solutions except for the publication (#2 – #9) include 3 m/s jitter

[a] McCarthy et al., 2004, ApJ 617, 575M
[b] $m_{\rm p_1} \cong 62.6 M_J$
[c] $m_{\rm p_1} \cong 79.47 M_J$
[d] $m_{\rm p_1} \cong 13.91 M_J$, $m_{\rm p_2} \cong 7.95 M_J$

viable solution, similar in that respect to #5 and possibly #7. The planetary masses in #9, are slightly larger than several Jupiter masses and the plane of orbit's orientation is nearly face on. The mass of the second planet in solution #8 is outside the range allowed by the KC model, as is the case with solution #7 (see §5.2).

6.2 Error Analysis and Fitness-Surface

The uncertainties for the quantities of solution #7 are shown in Table 6. These values were calculated by perturbing each of the solution's parameters and maintaining that changed value fixed during optimization. For each perturbation of a particular parameter, the search for the desired fitness value (χ^2 not normalized) was made on the entire remaining $(n-1)$-tuple. Here, the size of the desired confidence interval between the fitness value of the original minimum and that of the perturbed-optimized one was taken to be 1, corresponding to one standard deviation in the χ^2 function (i.e. optimizing to find $\chi^2_{\rm perturb} = \chi^2_{\rm original} + 1$). The smallest perturbation for which the fitness value changes as desired is considered to be the uncertainty for the perturbed pa-

Table 3. Uncertainties for the parameters of the reproduced Keplerian solution to the binary HD141929

Model Parameter (and unit)	– (negative side uncertainty)	Parameter value	+ (positive side uncertainty)	Published uncertainty (for comparison)
P_1 $(days)$	0.02	49.70	0.05	± 0.016
K_1 (ms^{-1})	400	9950	200	± 170
e_1	0.02	0.393	0.02	± 0.008
ω_1 (deg)	5.00	326	2.00	± 1.700
T_1 (days)	0.300	1993	0.300	± 0.190

Table 4. Results for the Binary system HD141929

Solution	P $(days)$	T_0 (HJD-2451000)	e	ω_1 (deg)	ω_2 (deg)	K_1 (m/s)	K_2 (m/s)	RMS [a] (m/s)	i (deg)	K_1/K_2
Published[bc]	49.70	993.39	0.393	325.7	145.7	9950	10580	562	~ 11	0.94
KC Primary[d]	49.71	993.40	0.403	324.7		9770		518		0.93
KC Secondary	49.69	993.40	0.412		145.2		10497	365		0.93
POFP fit #1[e]	49.69	992.90	0.386	320.7	140.7	9508	10119	535	10.74	0.94
POFP fit #2[f]	49.72	993.09	0.406	142.2	322.2	9556	10166	510	10.78	0.94

[a] For all generated solutions and reproductions in this table, RMS $= \sigma_{\mathrm{res}} = \sqrt{\mathrm{RMS}^2_{\mathrm{ERR}} + \sigma_{\mathrm{jit}^2}}$
[b] Simultaneous fit of both stars' RV data
[c] Carrier, 2002, A&A 389,475
[d] individual Keplerian fit (using the KC model)
[e] assuming $M_1 = 2.6M_\odot$ $M_2 = 2.445M_\odot$
[f] assuming $M_1 = 2.6M_\odot$ $M_2 = 2.445M_\odot$

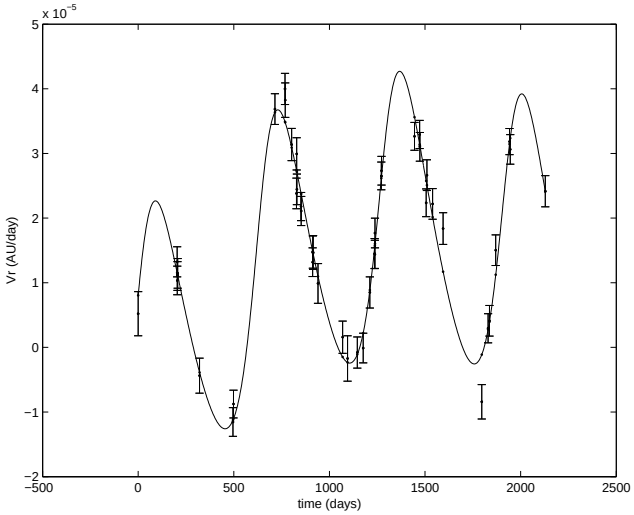

Figure 1. The RV fit for solution #7 in Table 1. The error bars include a jitter of 3 m/s.

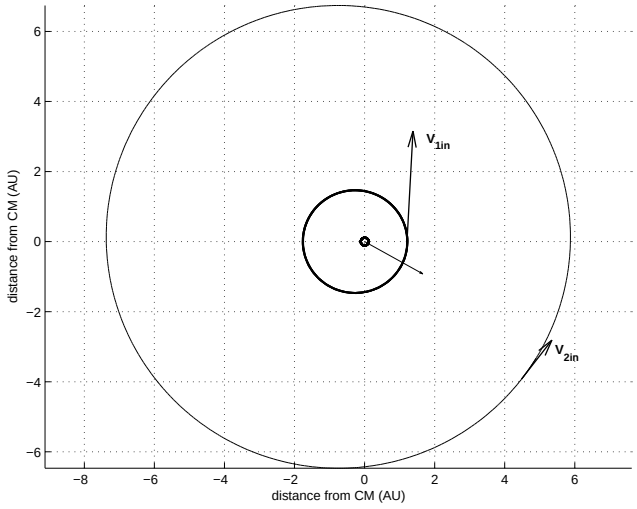

Figure 2. The trajectories of the system in solution #7, around the centre of mass (the star, at the centre, is marked in red, the inner planet is marked in blue and the outer planet in black), integrated over a time span of 1 period of the outer planet. The red arrow at the centre is the look-vector, pointing in the direction of the observer's line of sight. Also shown are the initial velocities for each planet

rameter. As was the case here, the search is typically made using the Compass Method. Based on "The use of constant Chi-Square Boundaries as Confidence Limits" in Press et al. (1992) and on Bevington & Robinson (2003), this approach results in an error analysis that examines how sensitive the solution is to a change in each variable. It quantifies the shape of parameter space around a solution (Windmiller 2006) and is not limited to a function resembling the one passing through the original data points (i.e. it reaches families of the original curve). Because of that such an analysis

Table 5. χ^2_ν intervals for different confidence levels using the F test with examples shown for HD160691 ($\nu = 34$)

Confidence:	2σ	$\frac{1}{F} \longleftarrow 1\sigma$	χ^2_ν	$\longrightarrow \mathrm{F}\ 1\sigma$	2σ
$\left\{\chi^2_\nu\right\}_{\min/\max} = \chi^2_\nu \times$	0.493	0.703		1.423	2.028
For solution #1:	1.310	1.860	2.650	3.770	5.370
For solution #2:	0.630	0.900	1.280	1.820	2.600
⋮			⋮		

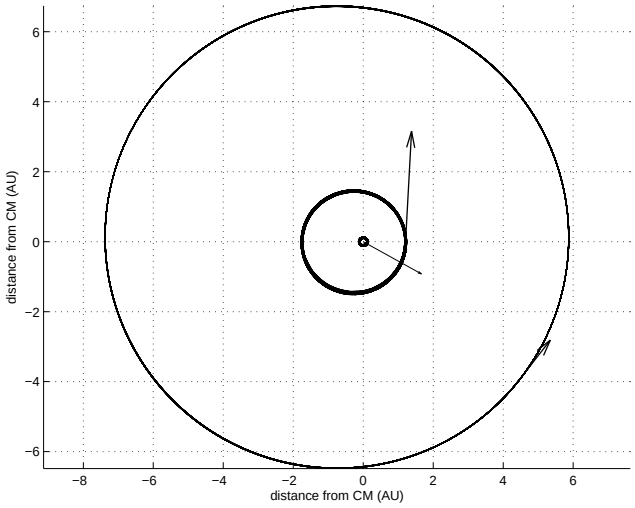

Figure 3. The trajectories of the system in solution #7, integrated over a time span of 400 periods of the outer planet (703 years), demonstrating its stability.

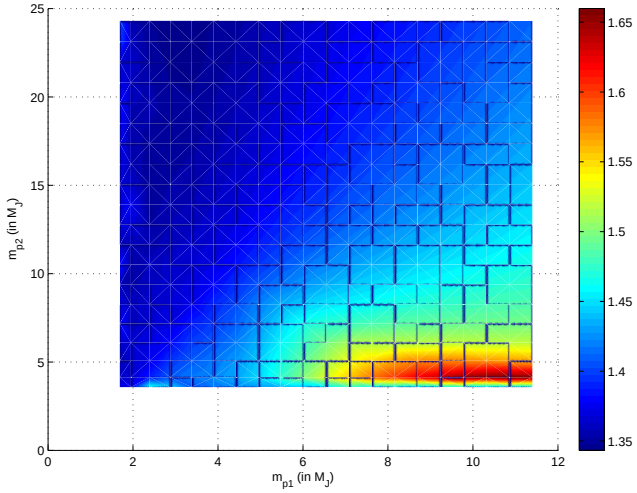

Figure 4. The surface $\chi^2_\nu = s\,(m_1, m_2)$, looking down the fitness axis, for HD160691. The fitness was calculated on a mass grid of $10 \times\ 10$ mass values. The fitness scale is shown as a colour bar on the right, with a minimum value of $\chi^2_{\nu_{\min}} = 1.35$.

can reflect properties of the set of parameters that otherwise require a different way of interpretation (Examples to that are shown in Windmiller (2006) and Paper II). It also stands in contrast to methods adding or redistributing Gaussian noise, such as the Monte Carlo, frequently used in the literature, which, in fact, tend to underestimate the error. Table 4 also shows the composite errors of quantities which include parameters of the basic 12-tuple in their expressions. These were calculated in closed form using the propagation of errors.

An analysis based on the translation from the published double Keplerian solution, into the POFP 12-tuple, was carried out by calculating the surface of fitness as a function of the two masses (or inclinations), for the lowest $\Delta\Omega$ in each grid-point (see §5.2 and Appendices C,E). Fig. 4 shows the surface, viewed along the χ^2_ν axis (in the origin's direction), where the different heights of the fitness are represented by a range of colours. Fig. 5 is a simplified contour plot of the main features shown in Fig 4. With the KC parameters used to generate Newtonian initial conditions for the **Solver**, the reproduced KC solution #2, with $\chi^2_{\nu\mathrm{Kep}} = 1.27$ now has a minimum, $\chi^2_{\nu\mathrm{Newt}} = 1.38$. The χ^2_ν values of the POFP solutions given in Table 1 are closely comparable to the best $\chi^2_{\nu\mathrm{Newt}}$ values derived from the KC parameters of #2. Because the masses derived in a POFP solution are only bounded by $m_{1,2} > 0$, they are not limited to the range set by the KC, allowing for a solution outside the region boxed by the fitness surface and the constant surface representing the single fitness value of #2. This point is discussed further in subsequent papers in the context of both fits for different stellar systems and stability analysis.

6.3 Discussion of HD160691 Results

Reconstructing planetary orbits by fitting RV measurements is an inverse problem, and as such, it is reasonable to expect multiple solutions that are consistent with the data. The variety of cases, $\#3 - \#9$, demonstrate the nature of the POFP operation as an attempt to solve this inverse problem, and the types of solutions it can produce. In the interpretation presented here, the fit for every solution is judged by the three criteria, in order: χ^2_ν, RMS, and stability. Only when considering all three, will the viability of a particular solution be realized. The interchange between stability and lower χ^2_ν is demonstrated, for example, in the differences between solutions #4, #5, #6, #7 increasing in stability with the RMS rising along with the χ^2_ν (dropping again for #7). As discussed in §5 and §6.1, the issue of stability is addressed by both direct integration and the Hill stability analysis. The Hill difference is apparent as a general trend but, depending on the actual value for a particular

Table 6. Uncertainties for the parameters of Solution #7

Model Parameter (and unit)	- (negative side uncertainty)	Parameter value	+ (positive side uncertainty)
m_1 (M_J)	0.100	1.76	0.500
m_2 (M_J)	0.500	3.03	0.900
m_3 ($M_\odot$)	0.080	1.08	0.200
x_1 (AU)	0.030	1.22	0.030
x_2 (AU)	0.300	5.77	0.300
y_2 (AU)	0.300	-1.15	0.600
z_2 (AU)	0.090	-0.48	0.090
θ_1 (rad)	0.009	-0.0655	0.009
θ_2 (rad)	0.090	-0.521	0.090
e_1	0.008	0.183	0.030
e_2	0.090	0.123	0.090
τ (rad)	–	set to $\tau = 0$	–
Composite Error:			
$m_1 \sin i_1$ (M_J)	0.10	1.60	0.50
$m_2 \sin i_2$ (M_J)	0.10	2.75	0.50
a_1 (AU)	0.07	1.50	0.07
a_2 (AU)	0.80	6.73	0.80
P_1 (days)	40	642	40
P_2 (days)	500	6130	500

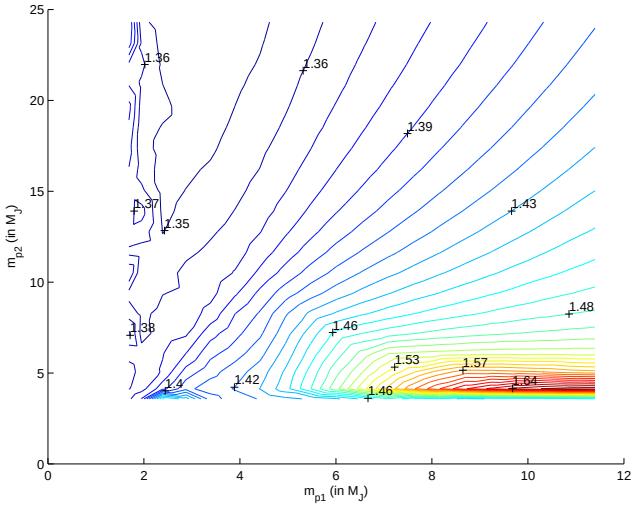

Figure 5. A contour representation of the main features of Fig. 4. As shown by the height labels, the denser concentrations of contour lines designate lower regions of χ^2_ν on the fitness surface (bluer regions in Fig. 4)

solution, may not be definite. The capacity for generality in the geometry of the POFP solutions is apparent in this regard by noting that solutions #5, #7, #6 are co-planar, nearly co-planar and completely three dimensional respectively. Solutions #3 and #6 demonstrate the same value of χ^2_ν, with the former being possibly unstable while the stability of the latter being well supported. This difference in stability, also shown by the respective RMS values, is possibly related to the large mass of the first planet occurring in #3 only. Following the arguments and methods presented in §5, §6.1, and in this section, the disparity between a Keplerian fit and a Newtonian fit is also expressed in the different values of their fitness function, assuming the same jitter effect (see also Fig. 4). In any event, a full consideration of all three criteria seems crucial in order to assess the acceptability of a model for a given solution and understand its implications. This full consideration is also necessary in order to compare between different solutions representing the same model and between different models. The observer's direction (expressed by the look-vector) can also be considered. Of the six solutions suspected of being stable (or at least semi stable), #3, #5, #6, #7, #8, #9, solutions #5 and #9 are nearly co-planar face on while #7 is nearly co-planar edge on. Solutions #3, #6, #8 are three dimensional. All of these solutions have eccentricity values smaller than 0.26. The lowest fit is that of the unstable solution #4 with $\chi^2_\nu = 1.34$. Generated for the same data set, it is interesting to note how diverse the solutions are, as the different observational orientations of #7 and #9 show.

Considering the dispersion across the variety of solutions over the periods shows that the inner period is well constrained (and in agreement with the literature and its reproduction). The outer period, however, is not. Of the six stable-suspected solutions mentioned above, #5, #8, #9 have similar outer periods, differing from those of #6 and #7 (which also differ from one another) and from the literature and reproduction. These facts also express the interconnected multitude of issues discussed in this paper, emanating from the structure of POFP, especially with relation to existing methods. Extending the time baseline of the observations to include sufficient data for a fit that may determine the period of the second planet will provide a distinction between POFP and other models. POFP fits based on such data (for example the HARPS data used in Pepe 2006) are discussed in subsequent publications.

Examining the features of the fitness surface provides an insight as to the relation between the Newtonian POFP

and the Keplerian (or KC) approximation. Of prime interest is the question of gravitational interaction in a physically realistic model. The significance of POFP in that regard, compared to other models, is expressed here in two ways. One is the variation in fitness across the (m_1, m_2) domain of the surface, compared to the fitness value provided by the Keplerian solution. For example, the $\chi^2_{\nu\mathrm{Kep}}$ value provided in #2 requires a specific range of masses in this domain. Alternatively, the values of $m \sin i$ provided by #2 correspond on the surface to higher values in $\chi^2_{\nu\mathrm{Newt}}$ than the $\chi^2_{\nu\mathrm{Kep}}$ tabulated. The gap between the POFP and the Keplerian model is also exhibited with solutions existing outside the allowable Keplerian mass region and have a reasonable χ^2_ν, RMS, and are stable (for example, #7 in Table 1). The high RCS and RMS of most of the POFP orbits (represented by the points of the surface) indicate that mutual planetary interaction plays a crucial role in considering the physics behind the models and in any comparison between them. The fact that viable POFP solutions, with masses not allowed in the Keplerian parameter space, exist, further emphasizes this point.

7 FUTURE WORK

The use of fundamental physical principles while preserving generality - physical, geometrical, and structural - allows the production of orbital solutions by POFP that are diverse, yet physically realistic. As demonstrated by the HD160691 analysis, the use of the POFP, especially considering the variety of independent optimisation methods it is structured around, raises some interesting issues. Perhaps the most distinct of those is the acceptability of the multiple (here, double) Keplerian model. On the one hand, comparison between the POFP and the Keplerian (or KC) predictions leads to the question of what constitutes sufficient viability of any model with respect to observations and also in comparison to another model. Considerations concerning the conditions for measuring a fit and the interpretation accompanying these conditions are highly valuable in assessing a comprehensive realistic description of natural phenomena. This issue has been expressed in this research with the requirement for making a wise use of the χ^2 and with arguments, such as the ones discussed earlier, regarding the necessity of the triple criteria for the acceptance of a fit (χ^2, RMS and stability). These considerations demonstrate a discussion concerning the foundation of scientific explanations. On the other hand, from a physical standpoint, the analysis of POFP solutions or a comparison between those and their Keplerian counterparts is linked to the question of gravitational interaction between multiple orbital elements, such as planets. The translation of KC into Newtonian information suggests that the former may be incomplete, regardless of the question of compatibility with the observed quantities.

In light of attempting to address those issues, at least two directions of utilizing the POFP will follow. One use is the study of other stellar systems suspected of including planets. An example of that is the investigation, relating to the existing literature, of RV data for 47 UMa and HD12661, which will appear in Paper II (and is also based on the existing investigation in Windmiller (2006)). Such studies are not limited to Three-Body configurations as an analysis of the suspected multiple-planetary system ρ Cancri A, on Paper III, will show. The other avenue in which the POFP can be used constructively is the vast topic of stability. Assessing instability in each solution via a full Three-Body integration is computationally expensive, while short time-span integration can only hint at such a possibility. Thus, the preliminary check for instability (though it may rely on founded criteria such as the Hill condition) like the one described for each solution here, must be expanded into a consistent methodical set of tools allowing for a rigorous analysis. A more thorough study of stability, based in part on the fitness surface described above and that may possibly point in a systematic direction, will be described in a future paper.

ACKNOWLEDGMENTS

The research reflected in this paper and the effort of writing and bringing it to print has been made possible through the constant support of the San Diego State University Astronomy department. In particular, we'd like to thank Dr. Fred Talbert for his relentless efforts of thorough commentation on drafts of this paper and the thesis work preceding it.

REFERENCES

Bevington P. R., Robinson D. K., 2003, Data Reduction and Error Analysis, 3rd ed. New York: McGraw-Hill, NY
Fischer D. A., Marcy G. W., Butler R. P., Laughlin G., Vogt S. S., 2002, ApJ, 564, 1028
Gladman B., 1993, Icarus, 106, 247
Goździewski K., Maciejewski A. J., 2003, ApJ 586, L153
Hilditch R. W., 2001, An Introduction to Close Binary Stars, 1st ed. Cambridge University Press, Cambridge, UK
Kolda T. G., Lewis R. M., Torczon V., 2003, Siam Review, 45, 385
Laughlin, G., Chambers J.E., 2001, ApJ, 551, L109-L113
Marchal C., Bozis G., 1982, Celestial Mechanics, 26, 311
McCarthy C. Butler P. R., Tinney C. G., Jones H. R. A., Marcy G. W., Carter B., Penny A. J., Fischer D. A., 2004, ApJ 617, 575M
Nautical Almanac Office, 2006, The Astronomical Almanac. US Government Printing Office. Washington DC.
Naef D., Mayor M., Beuzit J. L., Perrier C., Sivan J. P., Udri S., 2004, A&A, 414, 351
Pepe F. et al. 2006, A&A, 462, 769P
Press W. H. et al., 1992, Numerical Recipes in Fortran, 2nd ed. New York: Press syndicate of the University of Cambridge.
Rivera E. J., Lissauer J. J., Butler R. P., Marcy G. W., Vogt S. S., Fischer D. A., Brown T. M, Laughlin G., Hanry G. W., 2005, ApJ 634, 625
Shampine L. F., Gladwell I., Thompson S., 2003, Solving ODEs with MATLAB, 1st ed. Cambridge University Press, Cambridge, UK
Windmiller G., 2006, Master Thesis, San Diego State University.
Wright J. T., 2005, PASP, 117, 657W

APPENDIX A: INITIAL POSITIONS IN THE PLANETARY MODEL

In the orbital planes of masses m_1 and m_2 around mass m_3, the initial position of each mass in orbit is:

$$\boldsymbol{s}_{e1} = \frac{a_1\,(1-e_1)}{1+e_1\cos\theta_1}\,(\cos\theta_1, \sin\theta_1, 0)\,, \qquad \boldsymbol{s}_{e2} = \frac{a_2\,(1-e_2)}{1+e_2\cos\theta_2}\,(\cos\theta_2, \sin\theta_2, 0) \tag{A1}$$

respectively. The initial velocity of each mass in orbit is:

$$\boldsymbol{v}_{e1} = \sqrt{\frac{G\,(m_1+m_3)}{a_1\,(1-e_1)}}\,(-\sin\theta_1, e_1+\cos\theta_1, 0)\,, \quad \boldsymbol{v}_{e2} = \sqrt{\frac{G\,(m_2+m_3)}{a_2\,(1-e_2)}}\,(-\sin\theta_2, e_2+\cos\theta_2, 0) \tag{A2}$$

The semi-major axes $a_{1,2}$ are given by the eccentricities $e_{1,2}$ and the coordinates of the periastra, (x_1) and (x_2, y_2, z_2) respectively.

$$a_1 = \frac{|x_1|}{1-e_1}, \qquad a_2 = \frac{\sqrt{(x_2^2+y_2^2+z_2^2)}}{1-e_2} \tag{A3}$$

The periods of orbit are given by:

$$P_{1,2} = \sqrt{\frac{4\pi^2 a_{1,2}^3}{G\,(m_3+m_{1,2})}} \tag{A4}$$

The rotation matrices used for the transformation are:

$$\mathbf{R}_\psi = \begin{pmatrix} \cos\psi & -\sin\psi & 0 \\ \sin\psi & \cos\psi & 0 \\ 0 & 0 & 1 \end{pmatrix}, \quad \mathbf{R}_\eta = \begin{pmatrix} \cos\eta & 0 & -\sin\psi \\ 0 & 1 & 0 \\ \sin\eta & 0 & \cos\eta \end{pmatrix}, \quad \mathbf{R}_\tau = \begin{pmatrix} 1 & 0 & 0 \\ 0 & \cos\tau & -\sin\tau \\ 0 & \sin\tau & \cos\tau \end{pmatrix} \tag{A5}$$

where the angles are defined in terms of the second periastron coordinates, i.e.,

$$\cos\psi = \frac{x_2}{\sqrt{x_2^2+y_2^2}} \quad \text{etc.} \tag{A6}$$

The position and velocity vectors of all three bodies are then given as:

$$\boldsymbol{r}_{1\mathrm{in}} = \mathbf{R}_\psi\mathbf{R}_\eta\mathbf{R}_\tau\boldsymbol{s}_{e1}^T = (\boldsymbol{s}_{e1}, 0)\,, \quad \boldsymbol{r}_{2\mathrm{in}} = \mathbf{R}_\psi\mathbf{R}_\eta\mathbf{R}_\tau\boldsymbol{s}_{e2}^T, \quad \boldsymbol{r}_{3\mathrm{in}} = (0,0,0) \tag{A7}$$

$$\boldsymbol{v}_{1\mathrm{in}} = \mathbf{R}_\psi\mathbf{R}_\eta\mathbf{R}_\tau\boldsymbol{v}_{e1}^T = (\boldsymbol{v}_{e1}, 0)\,, \quad \boldsymbol{v}_{2\mathrm{in}} = \mathbf{R}_\psi\mathbf{R}_\eta\mathbf{R}_\tau\boldsymbol{v}_{e2}^T, \quad \boldsymbol{v}_{3\mathrm{in}} = (0,0,0) \tag{A8}$$

The 12-tuple of orbital parameters required to generate these initial conditions in the **Solver**'s frame is therefore $\boldsymbol{C_1} = (m_1, m_2, m_3, x_1, x_2, y_2, z_2, \theta_1, \theta_2, e_1, e_2, \tau_1)$.

APPENDIX B: TRANSFORMATION THROUGH THE PLANE OF THE SKY

The **Solver** receives the initial conditions, $\boldsymbol{C_1}$, specified in the previous section and produces the Three-Body trajectories and velocities in the form of the solution matrix *xyz* for time step t_k

$$[\textbf{Solver } \textit{coordinates}]_{t_k} \equiv \mathbf{xyz}_{t_k} = \begin{pmatrix} \bar{x_1} & \dot{\bar{x}}_1 & \bar{x_2} & \dot{\bar{x}}_2 & \bar{x_3} & \dot{\bar{x}}_3 \\ \bar{y_1} & \dot{\bar{y}}_1 & \bar{y_2} & \dot{\bar{y}}_2 & \bar{y_3} & \dot{\bar{y}}_3 \\ \bar{z_1} & \dot{\bar{z}}_1 & \bar{z_2} & \dot{\bar{z}}_2 & \bar{z_3} & \dot{\bar{z}}_3 \end{pmatrix}_{t_k} \quad , \; t_k = t_0 \to t_{final} \tag{B1}$$

(the bar represents a coordinate in the CM frame)

One of the masses, typically m_3, is chosen to be the star. Its velocity, $\boldsymbol{v_3} = \left(\dot{\bar{x}}_3, \dot{\bar{y}}_3, \dot{\bar{z}}_3\right)_{t_k}$ is extracted from the solution matrix.

The observer's line of sight, or radial direction, is designated by the z' axis which is perpendicular to the observer's plane of the sky. The orientation of the **Solver**'s solution to the observer is defined by one of the orbits chosen. The angles defining the transformation are the orbit's longitude of periastron, ω and inclination i, i.e. the 2-tuple $\boldsymbol{C_2} = (i, \omega)$. The appropriate transformation matrices are the following (Hilditch 2001):

$$\mathbf{R}_i \equiv \begin{pmatrix} \sin i & 0 & \cos i \\ 0 & 1 & 0 \\ -\cos i & 0 & \sin i \end{pmatrix}, \quad \mathbf{R}_\omega \equiv \begin{pmatrix} \cos\omega & \sin\omega & 0 \\ -\sin\omega & \cos\omega & 0 \\ 0 & 0 & 1 \end{pmatrix} \tag{B2}$$

and the transformation is:

$$\boldsymbol{v}_{r*}(t_k) = \mathbf{R}_i\mathbf{R}_\omega\boldsymbol{v}_3(t_k)^T = \mathbf{R}_i\mathbf{R}_\omega \begin{pmatrix} \dot{\bar{x}}_3 \\ \dot{\bar{y}}_3 \\ \dot{\bar{z}}_3 \end{pmatrix}_{t_k} \tag{B3}$$

The velocities of equation B3 for all time steps are then compared to the observations through the fitness function of the χ^2.

APPENDIX C: THE LOOK VECTOR

The solution produced by the **Solver**, given the orbital 12-tuple of initial conditions, $\boldsymbol{C_1}$, is in the form of the matrix

$$\boldsymbol{v}_{r*}(t) = \begin{pmatrix} \left(\dot{x_3}, \dot{y_3}, \dot{z_3}\right)_0 \\ \vdots \\ \left(\dot{x_3}, \dot{y_3}, \dot{z_3}\right)_k \\ \vdots \\ \left(\dot{x_3}, \dot{y_3}, \dot{z_3}\right)_f \end{pmatrix} \text{ corresponding to the time step vector } \boldsymbol{t} = \begin{pmatrix} t_0 \\ \vdots \\ t_k \\ \vdots \\ t_f \end{pmatrix}$$

The observer-orientation from which the RV data is optimally described can be solved for. In the equation

$$\mathbf{v}_{r*}\boldsymbol{L}_{i,\omega} = \boldsymbol{V}_O \tag{C1}$$

$\boldsymbol{V}_O = \begin{pmatrix} V_{o1} \\ V_{o2} \\ \vdots \\ V_{of} \end{pmatrix}$ is the vector of observed RV and $\boldsymbol{L}_{i,\omega} = \begin{pmatrix} \cos i \cos\omega \\ \sin i \sin\omega \\ \cos i \end{pmatrix}$ is a 'look-vector' which designates a particular point on a unit sphere (this point could be thought of as the direction where the line of sight leads to the observer). Because $\mathbf{v}_{r*}$ is not a square matrix, the singular value decomposition (the MATLAB function *svd*) provides a convenient calculation of the least squares solution to this over-determined system. The *svd* command provides the decomposition $\mathbf{v}_{r*} = \mathbf{QSP}^T$. With n being the number of rows in $\mathbf{v}_{r*}$, $\mathbf{Q}$ is an $n \times n$ orthogonal matrix, $\mathbf{P}$ is a 3×3 orthogonal matrix and $\mathbf{S}$ is a diagonal $n \times 3$ matrix. The matrix $\mathbf{S}^{-1}$ is constructed as a matrix of zeros, with three diagonal elements which are the reciprocals of the elements in $\mathbf{S}$. The look-vector is solved for as

$$\boldsymbol{L}_{i,\omega} = \mathbf{PS}^{-1}\mathbf{Q}^T\boldsymbol{V}_O$$

From the look-vector, i and ω (i.e. the components of the directional initial conditions 2-tuple, the vector $\boldsymbol{C}_2$) are obtained.

APPENDIX D: χ^2 AS A FITNESS FUNCTION

Given the observed velocities $(V_O)_k$, their errors σ_k, the computed (predicted) velocities $(V_C)_k$ and the offset velocities $(V_S)_k$ along the indices $k = k_1, k_2 \ldots$ that divide the data set, the form used for the fitness function (χ^2) is:

$$f_{fit}\left(V_{O_k}, \sigma_k, V_{C_k}, V_{S_k}\right) = \sum_{k_1}\left[\frac{V_{O_{k_1}} - \left(V_{C_{k_1}} + V_{S_{k_1}}\right)}{\sigma_{k_1}}\right]^2 + \sum_{k_2}\left[\frac{V_{O_{k_2}} - \left(V_{C_{k_2}} + V_{S_{k_2}}\right)}{\sigma_{k_2}}\right]^2 + \ldots \tag{D1}$$

The indices are determined by the number of different instruments used to obtain the observations. The total number of entries (k, or the number of indexed points $k_1 + k_2 + \ldots$), on which the summation in Equation D1 is made, is the number of data points. To optimize for the offset velocity, the partial derivatives of the fitness function are taken and set to zero:

$$\frac{\partial f_{\text{fit}}}{\partial V_{S_k}} = 2\sum_k\left[\frac{V_{O_k} - (V_{C_k} + V_{S_k})}{\sigma_k}\right]\left[\frac{1}{\sigma_k}\right] = 0 \Rightarrow \sum_k\left[\frac{V_{O_k} - V_{C_k}}{\sigma_k^2}\right] = \sum_k\frac{V_{S_k}}{\sigma_k^2}$$

arriving at the expression for the optimal offset correction

$$V_{S_k} = \frac{\sum_k\left[\frac{V_{O_k} - V_{C_k}}{\sigma_k^2}\right]}{\frac{1}{\sigma_k^2}} \tag{D2}$$

APPENDIX E: TRANSLATING A DOUBLE KEPLERIAN INTO POFP

In the following process, the standard notation for the orbital properties of binaries, expressed in Hilditch (2001), is used. The orbital-observational parameters characterizing an orbit in the Keplerian model are P, K, T, ω, e.

Given the times of first observation, t_{0_1}, t_{0_2}, the times of periastron passage for each planet, T_1, T_2 can be translated into the delay angles θ_1, θ_2 respectively. This can be done by using the Newton-Raphson method to iterate for the eccentric anomaly, E, in Kepler's Equation (3):

$$2\pi\frac{t_{0_{1,2}} - T_{1,2}}{P_{1,2}} = E_{0_{1,2}} - e_{1,2}\sin E_{0_{1,2}} \tag{E1}$$

The eccentric anomaly can then be used to solve for the true anomaly at time t_0 (4):

$$\theta_{1,2} = \theta(t_{0_{1,2}}) = 2\arctan\left[\sqrt{\frac{1+e_{1,2}}{1-e_{1,2}}}\tan\left(\frac{E_{0_{1,2}}}{2}\right)\right] \tag{E2}$$

The periastron position in the first-planet coordinate system is set on the positive x axis and therefore can be calculated from the period (A4):

$$a_{1,2} = \left[\frac{P_{1,2}^2 G\left(m_3 + m_{1,2}\right)}{4\pi^2}\right]^{\frac{1}{3}} \quad , \quad x_1 = a_1\left(1-e_1\right) = \frac{a_1\left(1-e_1^2\right)}{1+e_1\cos\theta_1(0)}\cos\theta_1(0) \tag{E3}$$

where the delay angle is $\theta_1(0) = 0$. The two masses are either given directly or can be calculated from the inclinations of the two orbits by use of the mass function (which is given and by the fitted half-amplitude velocity K, period P and eccentricity e):

$$f(m)_{1,2} = f(m_{1,2}) = \frac{P_{1,2}K_{1,2}^3}{2\pi G}\sqrt{1-e_{1,2}^2} \quad , \quad f(m)_{1,2}\left(m_{1,2}+m_3\right)^2 = m_{1,2}^3\sin^3 i_{1,2} \tag{E4}$$

where $m_{1,2}$ can be extracted from the expression on the right using a Newton-Raphson iteration.

The coordinates of the second periastron can be calculated using the relative positions of the two orbits' periastra. The rotation matrices used to transform the coordinate system of the first periastron to that of the second are:

$$\mathbf{R}_\omega = \begin{pmatrix} \cos\omega & -\sin\omega & 0 \\ \sin\omega & \cos\omega & 0 \\ 0 & 0 & 1 \end{pmatrix}, \quad \mathbf{R}_i = \begin{pmatrix} 1 & 0 & 0 \\ 0 & \cos i & -\sin i \\ 0 & \sin i & \cos i \end{pmatrix}, \quad \mathbf{R}_\Omega = \begin{pmatrix} \cos\Omega & -\sin\Omega & 0 \\ \sin\Omega & \cos\Omega & 0 \\ 0 & 0 & 1 \end{pmatrix} \tag{E5}$$

with $\Omega_{1,2}$ being the position angle of the nodal point in each orbit.
The transformation is then:

$$\begin{pmatrix} x_2 \\ y_2 \\ z_2 \end{pmatrix} = \mathbf{R}_{-\omega_1}\mathbf{R}_{-i_1}\mathbf{R}_{-\Omega_1}\mathbf{R}_{\Omega_2}\mathbf{R}_{i_2}\mathbf{R}_{\omega_2}\begin{pmatrix} a_2(1-e_2) \\ 0 \\ 0 \end{pmatrix} = \mathbf{R}_{-\omega_1}\mathbf{R}_{-i_1}\mathbf{R}_{(\Omega_2-\Omega_1)}\mathbf{R}_{i_2}\mathbf{R}_{\omega_2}\begin{pmatrix} a_2(1-e_2) \\ 0 \\ 0 \end{pmatrix} \tag{E6}$$

Finally, the tilt τ, of the second orbit, relative to the first, is calculated via the same transformation, using the third component of the vector:

$$\boldsymbol{\tau} = \mathbf{R}_{-\omega_1}\mathbf{R}_{-i_1}\mathbf{R}_{(\Omega_2-\Omega_1)}\mathbf{R}_{i_2}\mathbf{R}_{\omega_2}\begin{pmatrix} 0 \\ 1 \\ 0 \end{pmatrix} \quad , \quad \tau = \frac{\arctan\left(\boldsymbol{\tau}_z\right)}{\sqrt{1-\left(\boldsymbol{\tau}_z\right)^2}} \tag{E7}$$

The look-vector can also be calculated with a transformation using the same rotation matrices:

$$\boldsymbol{L}_{i,\omega} = \mathbf{R}_{-\omega_1}\mathbf{R}_{-i_1}\begin{pmatrix} 0 \\ 0 \\ -1 \end{pmatrix} \tag{E8}$$

This paper has been typeset from a TEX/ LATEX file prepared by the author.